*JECT. 2008;40:175–183*
*The Journal of ExtraCorporeal Technology*

# Evaluation of the Doppler Technique for Fat Emboli Detection in an Experimental Flow Model

Victoria Wikstrand, MSc; Nadja Linder, MSc; Karl Gunnar Engström, MD, PhD, FRCS

*Heart Centre, Cardiothoracic Division, Department of Surgical and Perioperative Sciences, Northern University Hospital, Umeå, Sweden*

**Abstract:** Pericardial suction blood (PSB) is known to be contaminated with fat droplets, which may cause embolic brain damage during cardiopulmonary bypass (CPB). This study aimed to investigate the possibility to detect fat emboli by a Doppler technique. An in vitro flow model was designed, with a main pump, a filter, a reservoir, and an injector. A Hatteland Doppler probe was attached to the circulation loop to monitor particle counts and their size distribution. Suspended soya oil or heat-extracted human wound fat was analyzed in the model. The concentrations of these fat emboli were calibrated to simulate clinical conditions with either a continuous return of PSB to the systemic circulation or when PSB was collected for rapid infusion at CPB weaning. For validation purpose, air and solid emboli were also analyzed. Digital image analysis was performed to characterize the nature of the tested emboli. With soya suspension, there was an apparent dose response between Doppler counts and the nominal fat concentration. This pattern was seen for computed Doppler output ($p = .037$) but not for Doppler raw counts ($p = .434$). No correlation was seen when human fat suspensions were tested. Conversely, the image analysis showed an obvious relationship between microscopy particle count and the nominal fat concentration ($p < .001$). However, the scatter plot between image analysis counting and Doppler recordings showed a random distribution ($p = .873$). It was evident that the Doppler heavily underestimated the true number of injected fat emboli. When the image analysis data were subdivided into diameter intervals, it was discovered that the few large-size droplets accounted for a majority of total fat volume compared with the numerous small-size particles (<10 μm). Our findings strongly suggest that the echogenecity of fat droplets is insufficient for detection by means of the tested Doppler method. **Keywords:** fat emboli, cardiopulmonary bypass, Doppler, brain damage. *JECT. 2008;40:175–183*

Cerebral injury is a serious complication in cardiac surgery. Two types of injury are discussed. Type 1 mostly reflects cerebral macroemboli that may cause focal neurologic damages, typically stroke (1). Type 2 is usually described as impaired neurocognition and may have a multifactorial background. One mechanism behind the type 2 injury suggests microembolization of fat particles from retrieved pericardial suction blood (PSB) (2). Fat deposits have been observed in the cerebral microcirculation, described as "small capillary and arteriolar dilatations" (SCADs) (3). SCADs are associated with the recycling of PSB (4). Type 2 is very common, with a reported incidence of between 3% and 80%, depending on observational methods used (5,6). This is in contrast to type 1 injury, with a reported incidence of between 1.6% and 4.6% after routine procedures (7,8).

Address correspondence to: Karl Gunnar Engström, Heart Centre, Cardiothoracic Division, Department of Surgical and Perioperative Sciences, Northern University Hospital, S-90185 Umeå, Sweden. E-mail: gunnar.engstrom@vll.se
The authors have no conflict of interest regarding the presented data, with no commercial funding or industrial involvement. In more general terms of cardiac surgery, Karl Gunnar Engström reports a consultancy contact with AstraTech AB, Mölndal, Sweden regarding blood handling.

Microemboli are possible to detect by means of transcranial Doppler (9), and multifrequency devices may differentiate between solid and gaseous microemboli (10). The methodology is complex, and new algorithms were developed (11). The automated algorithms are partly user-specific in the hands of different operators (12). In cardiac surgery in particular, the microemboli are heterogeneous in their nature, and it remains a challenge to understand these phenomena in terms of Doppler signals (13). The Doppler technology seems mainly occupied with the intriguing differentiation between solid and gaseous emboli, whereas it is uncertain whether the Doppler can discriminate and detect fat emboli. This is in view of the unknown echogenicity and acoustic impedance of fat droplets, a question that to our knowledge has not been well elucidated. Nevertheless, transcranial Doppler methods were recently used for this particular purpose in two clinical randomized trials. In these trials, type 2 damage was analyzed comparing PSB fat removal by cell-saver washing vs. the conventional recycling of the blood (14,15).

In view of the above, the question of interest is whether fat emboli are detected by ultrasound and how these particles are interpreted in size. Our study describes an experimental approach to this question. We designed a flow

model into which various forms of emboli were introduced and analyzed using a 1.5-MHz Hatteland pulsed Doppler. The Doppler response to suspended droplets of soya oil or human liquid fat was compared with digital image analysis, which characterized the embolic nature of the tested particles. The model was validated by air and solid particles. The embolic load of fat was calibrated to simulate surgical conditions, when PSB is continuously recycled to the systemic circuit or when PSB is collected during CPB to become rapidly infused at weaning.

## MATERIALS AND METHODS

### Embolic Models

The experimental model of fat embolization simulated the response when PSB was returned to the systemic circulation. Two extremes were studied (A) PSB was continuously recycled to the main circulation, which yields a low final fat concentration in the aortic line. (B) PSB was collected during CPB to be rapidly returned to the main circulation at the end of the procedure, which yields a high but transient fat concentration. Values on PSB volumes and fat amounts were from the literature (16). Condition A presumed that 418 mL of PSB, holding 1.53 mL of contaminating fat (16), was continuously recycled during a 60-minute CPB period at 5 L/min systemic flow rate. This model corresponded to $5.09 \times 10^{-4}$% of fat in the aortic line. Condition B presumed that the same amount of fat and PSB was collected during CPB to become retransfused during a 1-minute period at weaning. This mixing corresponded to $2.82 \times 10^{-2}$% of fat in the aortic line. For dose–response measurements, three additional fat concentrations were tested in linear scale concentrations between the two extremes: A and B. For validation purpose, air and solid emboli were tested as described below.

### Preparation of Fat Emboli

Two types of fat were tested: soya oil (E-quality; Apoteksbolaget AB, Göteborg, Sweden) and human liquid fat. Discarded pericardial fat was retrieved from two routine cardiac surgery patients. Liquid fat was heat extracted at 210°C for 10 minutes, followed by cooling and decanting. The fat was deposited inside a 1-mL syringe to be transferred by a three-way stopcock to a 10-mL syringe filled with vehicle, typically water unless otherwise specified. The smaller syringe was replaced with another 10-mL syringe and the fat mixture was suspended over the stopcock channel during 10 transfer cycles in between the two syringes. Air-free conditions were strictly ensured.

### Preparation of Air and Solid Emboli

The flow model (see below) was specially designed to disintegrate injected air into small bubbles. However, in this mode with air directly injected into the circulation loop, the true diameter of the air bubbles was not measurable by image analysis. To overcome this problem, stable air bubbles were needed. Echocardiographic contrast medium was tested (Sonovue; Bracco Diagnostics, Milan, Italy) but was found to create very small air bubbles below the detection level of the Doppler. In fact, this finding was predicted in view the purpose with this contrast medium. Low-molecular weight Dextran or bovine serum albumin was evaluated for bubble production, although these were found unstable. As an alternative, shaving foam was tested, mixed at 1:1 ratio with water. These bubbles were reasonably stable for image analysis and embolic measurements.

Different forms of solid emboli were analyzed. In addition to glass spheres used for Doppler calibration as described below, calcified debris was also tested. For this purpose, aortic valves were retrieved from two subjects undergoing valve replacement for stenotic disease. The valves were crushed and suspended in saline. Particles >200 μm were removed by filtration.

The effect of background noise from blood cells was studied. Blood was collected from a discarded mediastinal drain of a routine CABG patient, and the hematocrit was set to 33%. Heparin, 10 IU/mL, was added, and the blood was pre-filtered (40 μm). In these experiments, fat was suspended in the blood, and the medium within the circulation loop was supplemented with 9 g/L NaCl to avoid hemolysis.

### Patients

Overall, biological material was collected from five routine male cardiac surgery patients, with an average age of 71.4 ± 3.8 years. The tissue was retrieved after surgery and was not removed for experimental purpose. No patient identity was disclosed at sampling nor documented within the study. With the collected tissue, only information about sex, age, and type of surgery was recorded. This sampling procedure does not require ethical approval according to Swedish legislation, a procedure that was confirmed and agreed by the ethical review board.

### In Vitro Flow Model

A circulation loop was designed in which a Doppler recorder was positioned. In principle, the loop had a main pump (Polystan Modular; Polystan AS, Vaerlose, Denmark), a medium reservoir with de-airing properties from a water-lock mechanism (modified Fatcher PSB reservoir; AstraTech AB, Mölndal, Sweden), and a .2-μm filter unit (pre-bypass filter, by PALL Scientific, NY or by MAQUET AG, Rastatt, Germany). Defined emboli were loaded into an injector in connection with the circulation loop. The injector was under control by a peristaltic pump (Ismatec IPC; Labinett, Göteborg Sweden). All experiments were conducted at 37°C. The system is further described and is schematically shown in Figure 1.

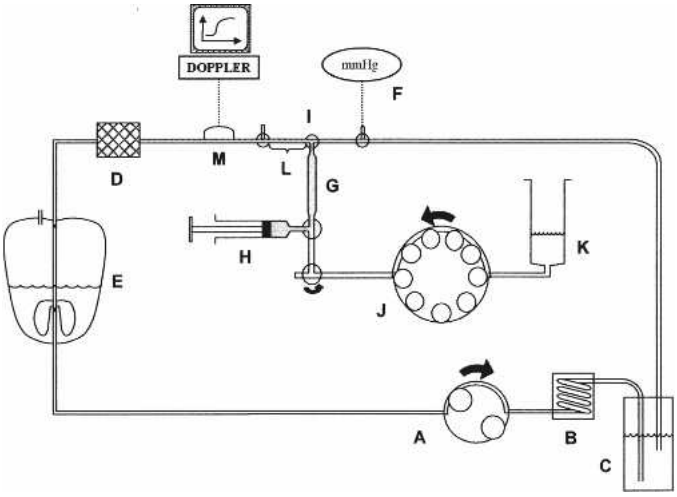


**Figure 1.** Schematic illustration of the flow model. A circulation loop was created using a main pump (A), a heat exchanger (B), a pressure equalizer and bubble trap (C), a .2-μm pre-bypass filter (D), and a medium reservoir equipped with an additional bubble trap of water-lock design (E). The circuit had a digital pressure recorder (F). Emboli of different characteristics, typically fat suspension, were introduced into the circuit in a standardized fashion. An injector cannula of determined volume 150 μL (G) was connected to the circuit. The injector was loaded with defined emboli by a syringe (H). Several stopcocks controlled the loading (exemplified at I). At experimentation, a peristaltic pump (J) pushed the emboli into the main circuit. The peristaltic pump used medium from a separate reservoir (K). At the injection point, a special design chamber helped to mix the emboli with the systemic flow (L). In the immediate vicinity to the injection point, a Doppler probe (Hatteland) was positioned (M). The temperature was calibrated and maintained by the heat exchanger (B) and a water bath in which the bubble trap (C) was positioned.

The main pump was calibrated (.290 L/min) to generate a .60 m/s flow velocity at the Doppler detection point, which corresponded to the blood velocity in the middle cerebral artery (17), an artery used for transcranial Doppler measurements. The injector pump was set at 881 μL/min, which emptied the embolic source (150 μL) into the circulation loop during a 10.2-second period while the Doppler signal was acquired. The fat concentration inside the injector was thoroughly calibrated against the known mixing between the injector flow and the main circulation flow to receive the desired nominal fat concentrations at the Doppler position.

The injection point was constructed to disintegrate air into small bubbles, and a design was selected by which the injection was perpendicular to the main flow. The injected air or particles entered a diffuser and a condenser that were made from two counter-positioned Luer adaptors that were located immediately before the tube section with the Doppler probe. The injector channel was vertically located and could be transposed to either an upward flow direction for experiments on air and fat emboli or a downward flow for solid particles. This was to compensate for sedimentation artifacts and to ensure a complete injection of the embolic material.

**Hatteland Doppler**

For embolic detection a pulsed Doppler was used (Hatteland CMD-10 and Bubmon-Detector software CM 03–06; HATTELAND Instrumentering, Royken Norway). The Doppler was equipped with a special design probe for the used type of tubing, 6.5-mm outer diameter (18), and was balanced for an appropriate measurement depth. The device was typically set at maximum sensitivity (0 dB), and the measurements cycle was 30 seconds, during which time the Doppler response to the injected emboli peaked and faded out. The device expresses both raw and computed data, the latter expressing a correction for shaded and extrapolated particles (deshading and deconvolution). This correction principle is not fully established (18), and therefore, raw data are here presented unless otherwise stated. The software subdivided the recorded data into nine particle-size intervals; 1 corresponding to small- and 9 to large-size particles within the selected sensitivity window.

The Doppler was calibrated according to the manufacturer's instructions using glass spheres. For this purpose, the flow circuit was modified to form a short recirculation loop. Before calibration, a Y-connector distributed the flow over the .2-μm filter and trap for de-airing. The tube section with the Doppler probe was vertically positioned to avoid sedimentation artifacts of the heavy glass spheres. The Doppler signal was measured at different concentrations of spheres and at different flow rates at 37°C. Under the microscope, the glass spheres had a diameter of 227.7 ± 10.0 μm, which was close to their nominal 200-μm size (Sigma Chemical, St. Louis, MO). This measurement considered all circular particles >20 μm, based on 10 repeated experiments. The calibration standard also contained dust particles of glass, <50 μm in diameter and of irregular shape, a finding that is in agreement with previous observations (19). The distribution curve is shown in Figure 2. The small-size dust particles are not assumed to

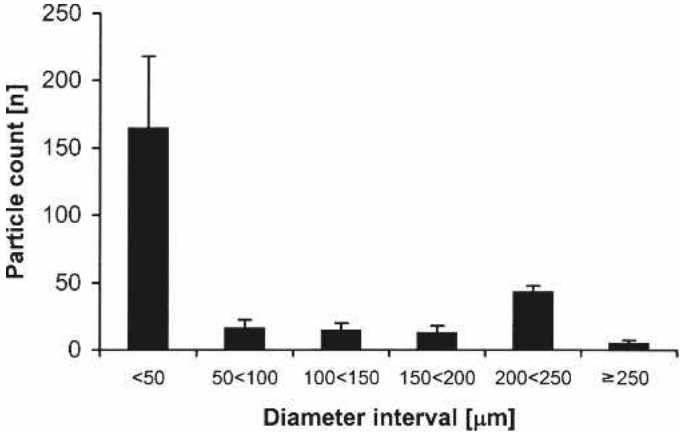


**Figure 2.** Size distribution of the glass spheres used for calibration. The spheres were suspended in water and were view under the microscope and image analysis (see text for further details). Mean ± SEM ($n$ = 10).

be visualized by the Doppler. According to the manufacturer's documentation, the Doppler response to the large-size glass spheres is equivalent to gas bubbles of ~40- to 50-μm diameter.

To exposed particles at a maximum Doppler resolution a cell-free medium was used, typically water with no additives. The integrated .2-μm pre-bypass filter cleared contaminating particles within the circulation loop, and before each experiment a particle free medium was confirmed by the Doppler. In all experiments, a control was run before the embolic test. These controls were identical to the emboli experiments, sharing the same preparation steps but with no particles added.

### Image Analysis and Processing

All Doppler experiments had a concomitant microscopy evaluation performed simultaneously but separated from the flow circuit. A multi-channel viewing chamber was designed based on a microscopy slide. Parallel pieces of Parafilm (118 μm thickness) were attached to the glass slide together with a coverslip roof. The sandwich was glued together by heat. The slide was positioned onto the stage of an inverted microscope (Olympus CK40; Olympus Optical, Tokyo, Japan) equipped with a phase contrast CDPlan ×10 objective lens, and recorded by a black and white camera (C5405-01; Hamamatsu Photonics, Hamamatsu City, Japan). A digital image analyzer (Zeiss, KS 300, version 3.0; Carl Zeiss Vision GmbH, Hallbergmoss, Germany) processed each image and presented the number of particles and their geometric characteristics. Data were transferred to an Excel worksheet programmed to separate particles into different diameter intervals. The program encountered all particles >3.5-μm-diameter cut-off. Inside the microscopy chamber, fat droplets were allowed to separate by density to accumulate and stabilize at the chamber top. Experiments on air bubbles followed the same procedure, whereas aortic valve particles collected at the bottom of the chamber. With this method, all contained particles were scanned into the image analyzer. Moreover, the camera input of the microscopic view corresponded to a certain volume of the chamber, calculated to be .0627 μL. This volume enabled calculation of the concentration of particles and their injected numbers into the Doppler flow model.

### Statistical Analysis

There is a linear expectancy between the incremental increase in nominal fat concentration and the number of identified particles by both the Doppler and the image analyzer. Nevertheless, because of scattered and skewed Doppler recordings correlations were analyzed by non-parametric Spearman rank test. Mean values ± SEM are given throughout; $p < .05$ was considered significant. SPSS version 14.0 was used (SPSS, Chicago, IL).

## RESULTS

### Model Evaluation

The flow model gave reproducible results. All experiments were initiated with a control of particle-free medium that had been handled in an identical fashion to the embolic preparations. Overall, the control measurements showed a mean particle count of 1.36 ± .32, suggesting a near particle and bubble-free preparation. Therefore, there was no need to correct individual experiments for background noise.

With injected air, the model gave bubbles in a wide range of diameters, with an apparent average in the segment between 100 and 200 μm. The Doppler software subdivided the recorded particles into nine diameter-size intervals within each of three levels of hardware sensitivity. Figure 3 shows detected air bubbles with the Doppler set at maximum (0 dB) sensitivity. With this setting, injected air showed a skewed distribution towards the right particle spectrum (e.g., large-size, corresponding to ~100 μm at interval 9). Shaving foam was used to create stable air bubbles that were possible to view under the microscope. These bubbles had a variable size with an averaged diameter of 45.7 ± 4.6 μm. The corresponding Doppler response is shown in Figure 3, which suggested a reasonable calibration. Ultrasound contrast medium (Sonovue) was tested as another form of stable air bubbles. However, these bubbles were too small to be identified by the Doppler (data not shown).

The solid nature of glass spheres used for calibration gave the expected Doppler output. In addition, suspended human valve calcifications were tested. With these solid particles, the Doppler identified 86 ± 33 counts (computed output), which was considerably less than the expected input. Microscopy showed that the preparation mostly resulted in small particles <10 μm in diameter (70.2%),

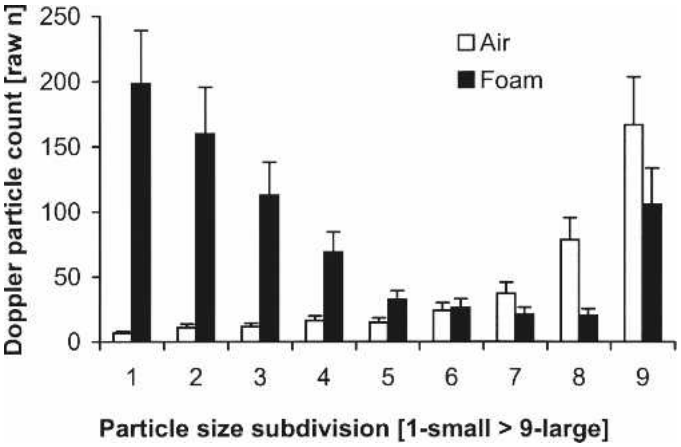


**Figure 3.** Particle counts subdivided into size intervals (1 through 9) as given by the Doppler device. The figure shows injection of air ($n = 10$) and foam ($n = 10$) into the flow model. The data refer to raw counts of the Doppler. Mean ± SEM.

which are not assumed to be detected by the Doppler. Nevertheless, the density of particles >20 μm was 12.8 ± 5.2/μL. The 150-μL embolic injector therefore delivered on average 1914 particles of this sort, the majority of which passed undetected by the Doppler.

**Embolic Fat Model**

Reproducible suspensions were created when soya oil or human fat was mixed with medium. The mixture had spherical particles of varying diameter. As expected, the particle density increased with higher fat concentrations. A typical microscopic view of human fat suspension is shown in Figure 4.

The Doppler indeed detected fat droplets when 150 μL of soya oil was injected. However, this procedure resulted in an unrealistically high concentration of fat compared with the prepared fat droplet suspensions that were tuned to simulate the surgical conditions during CPB. Moreover, it can be assumed that this approach formed droplets of very large size when the oil was dispersed inside the circulation loop. However, this assumption remains unknown as the droplets could not be visualized by microscopy in parallel with the flow model. The Doppler, on the other hand, mainly detected particles in the small-size spectrum (interval 1, Figure 5A). Conversely, when a corresponding volume of soya oil suspension was injected, the particles passed the Doppler virtually undetected. Figure 5A shows the recorded counts at the highest tested concentration of PSB fat contamination, according to model B. When the soya concentration was reduced, in a dose–response series, the recorded number of particles became even less, with virtually zero particles at the lowest concentration. In Figure 5B, concentrations 1 and 5 correspond to model A and model B, respectively. For raw Doppler data, a dose–response pattern could not be established ($p = .434$). However, for computed data, there was an apparent relationship between the fat dosage and the recorded particle count ($p = .037$; Figure 5B). It must be emphasized that this apparent relationship was based on extremely few Doppler-recorded particles (c.f. Figure 5A). In fact, with image analysis, the particle count was calculated and the number of fat droplets >20 μm that passed the Doppler probe was 105,251 ± 10,236 at the highest concentration (model B). If the numerous particles <20 μm were considered the discrepancy became even more remarkable. A corresponding Doppler dose–response experiment for human fat suspensions is shown in Figure 5C. A non-consistent relationship was observed ($p = .873$) for both raw and computed Doppler counts. Similar to the soya oil experiments, the Doppler severely underestimated the true number of injected particles observed under the microscope.

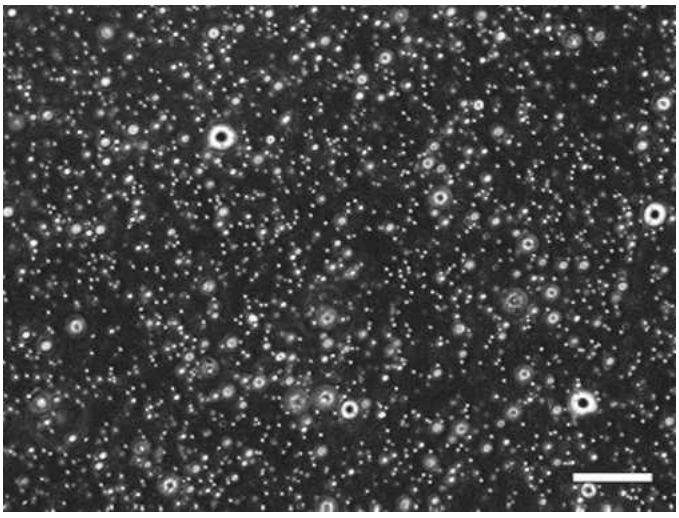

**Figure 4.** A typical microscopic view of human fat suspension to be injected into the flow model (intermediate fat concentration, type 3, see Materials and Methods for details). The bar corresponds to 100 μm.

The image analysis well discriminated the different fat concentrations, with a significant dose–response relationship between the nominal fat concentration and the recorded particle counts ($p < .001$; Figure 6A). However, when the Doppler response was plotted against the image analysis-derived count of injected particles, no obvious correlation was to be found (Spearman rho = –.059, $p = .686$; Figure 6B). The corresponding results from suspensions of soya oil resulted in a similar conclusion, by which the image analysis correlated well against the nominal fat concentration ($p < .001$), but there was no relationship against the Doppler count ($p = .168$).

**Blood Medium**

A parallel series of experiments was conducted in which human blood was used as vehicle for the fat suspensions. In control experiments without added fat ($n = 30$), the Doppler recorded 23.1 ± 3.0 particles. This finding showed a background noise from blood cells or their aggregates compared with the cell-free medium described above. When human fat was suspended in blood, the corresponding number of particles became surprisingly lower at 12.5 ± 4.36 ($n = 30$). The results refer to the average of three tested fat concentrations; according to low (model A), intermediate, and high (model B).

**Embolic Potential of Fat Particles**

The procedure to suspend fat mainly produced droplets of small size (Figure 7). However, when the volume of the individual particles was calculated, it became evident that the large particles accounted for the majority of fat volume. Therefore, even though the number of large fat particles was low, their embolic potential was pronounced compared with the more numerous small droplets. This phenomenon was seen for both soya oil and human fat suspensions (Figure 7). From the size distribution of par-

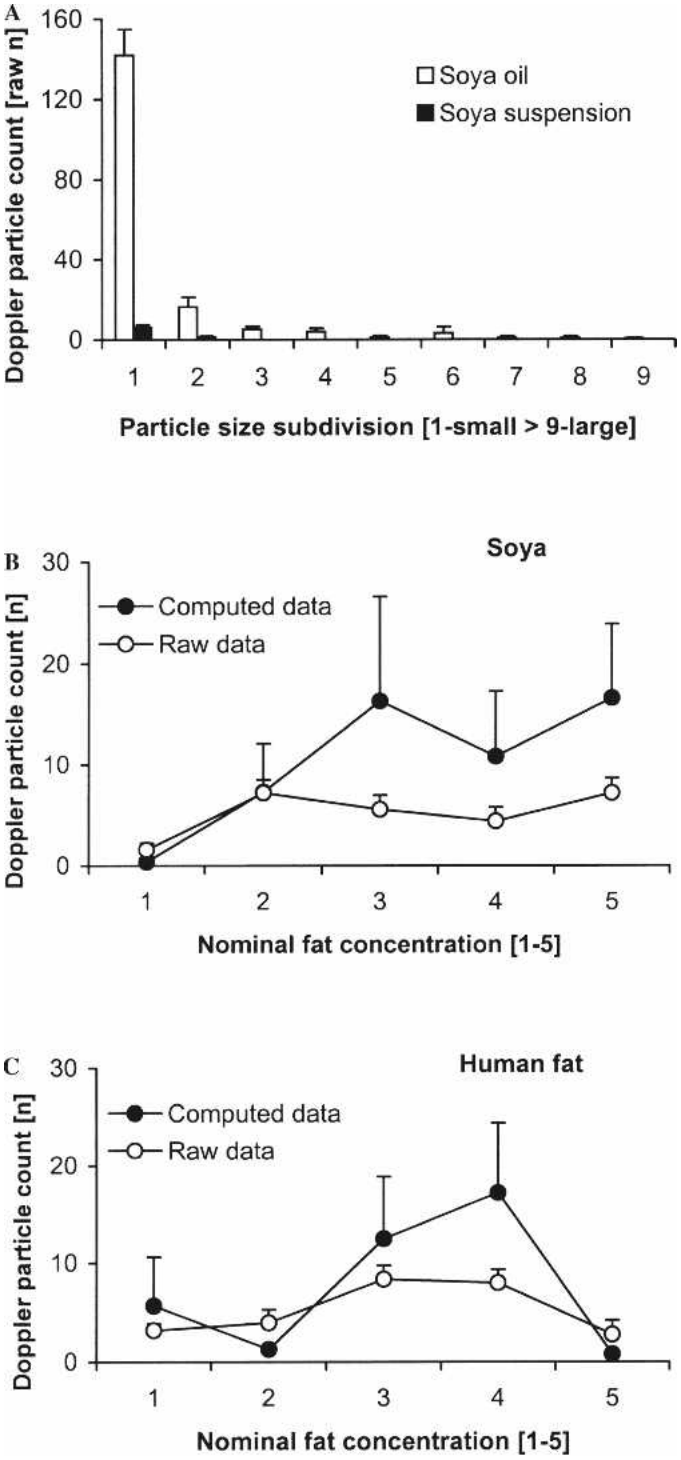


**Figure 5.** Doppler-recorded particles in response to injected fat. A, Raw Doppler counts during injection of 150 µL soya oil or soya-oil suspension at the highest tested concentration (type 5). The frequency distribution of particle size is seen with intervals 1 through 9, referring small to large particles. B, Doppler-detected particles vs. the nominal concentration of suspended soya oil. The vertical axis refers to the summation of Doppler counts from all size intervals 1 through 9, with both raw and computed data shown. Concentration of type 1 corresponds to model A and type 5 to model B. C, Doppler-detected particles vs. the nominal concentration of suspended human fat. The details are as in B. Mean ± SEM. $n$ = 10 for each concentration and type of fat.

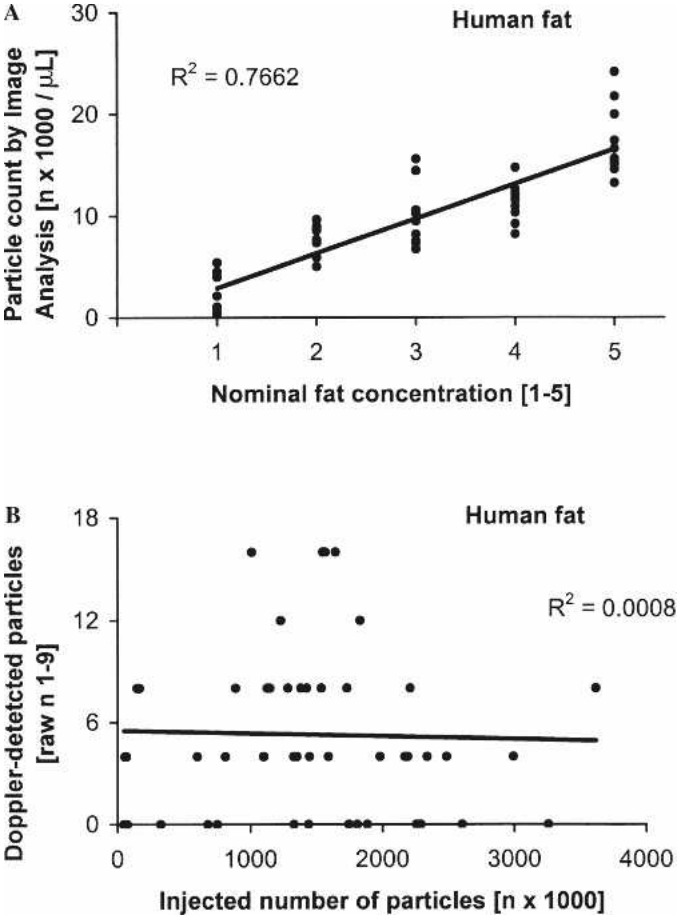


**Figure 6.** Dose–response patterns of human fat experiments; between the nominal fat concentration, particles detected by image analysis and Doppler, respectively ($n$ = 50). A, Particles counts measured by image analysis vs. the nominal concentration of suspended human fat. The indicated concentrations were identical to those referred in Figure 4B. B, Summation of Doppler raw counts vs. the injected number of particles as given by image analysis.

ticles, it is plausible to assume that the Doppler detects only the few large droplets. These Doppler-identified droplets are recorded as small-size particles (intervals 1 and 2), which correspond to air bubbles of ~10- to 30-µm diameter. Because of the very few Doppler-identified objects and the obvious diameter mismatch beyond the range, it was not meaningful to plot the particle size distribution against the corresponding image analysis data.

## DISCUSSION

Cardiac surgery is unfortunately associated with brain injury, typically subdivided into type 1 and type 2 damage (1). In part, this damage might be caused by cerebral embolization. For type 2 damage, different forms of emboli are discussed in the literature: solid, gaseous, and fat. Fat embolization was observed already in the early days of cardiac surgery (20,21). However, the problem with PSB

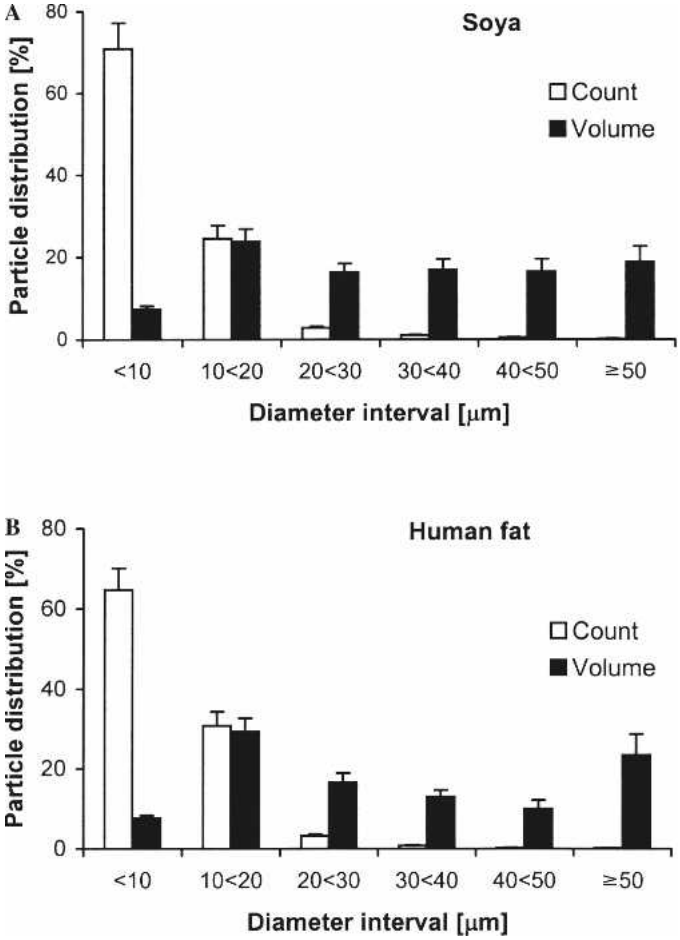


**Figure 7.** Frequency distribution of particle counts and the contained volumes of these particles with subdivision into diameter intervals as recorded by image analysis. A, Soya-oil suspension, $n = 50$. B, Human fat suspension, $n = 50$. Mean ± SEM.

fat contamination was assumed to have been overcome with the use of modern filters in the cardiotomy reservoir. During more recent years, the possible risks of fat embolism were re-emphasized when cerebral fat deposits were discovered. Such deposits were seen in patients who died shortly after cardiac surgery and in experimental animals undergoing operation with PSB recycling (4,22). The modern CPB equipment seems insufficient in its removal of PSB fat droplets (23). Instead, PSB must be processed by additive methods or be discarded to avoid the contamination. The cell-saver technology is considered very efficient in this respect (23). Other methods apply filtration (24) or spontaneous density separation together with surface adsorption (16).

It must be emphasized that the scientific relationship between cerebral fat embolization and type 2 damage remains to be elucidated. This hypothesis has thus far been tested in three randomized clinical trails among patients undergoing CABG, all using the cell-saver for PSB processing. In an early attempt from our research group, Svenmarker et al. (25) were unable to observe a benefit from use of cell-saver, based on 60 low-risk patients. A similar negative conclusion was recently derived by Rubens et al. (14), with neuropsychology testing of 247 routine patients. However, Djaiani et al. (15) tested the same hypothesis on 198 elderly patients and found a significant benefit from PSB fat removal. It is plausible to assume that all three studies were severely underpowered in view of the multifactorial and complex nature of type 2 damage. Of particular interest is the issue of elderly patients who may benefit more from PSB processing because of parallel cerebrovascular disease. Advanced age is commonly reported to be a dominating risk factor for different kinds of brain damage after cardiac surgery (26).

In the two recent studies referred above (14,15), transcranial Doppler was used with the ambition to monitor fat embolization. The transcranial Doppler is indeed an important method to visualize cerebral embolization (9), primarily with a focus on gaseous emboli. Modern CPB circuits are often equipped with in-line Dopplers (27). To what extent the Doppler actually visualizes fat droplets seems to be unknown. In fact, when the Doppler was used for this particular purpose in the two referred studies, no conclusive findings were obtained (14,15). This study was conducted to illuminate this issue. An in vitro flow and embolic model was developed with a tube-connected 1.5-MHz Doppler probe attached. Our aim was to verify Doppler detection of fat droplets and their size. A possible clinical implication from using this particular Doppler is to monitor fat embolization when stored volumes of PSB are re-transfused into the systemic CPB circuit. Nevertheless, the device cannot be assumed to discriminate between fat droplets and air bubbles. Our model was tuned to simulate clinical conditions when PSB is recycled back into the systemic circulation. Information about PSB volume and contaminating fat percentage during routine CABG procedures were derived from the literature (16). Two extremes were tested: PSB was continuously recycled back into the systemic circulation and PSB was collected during CPB to become re-transfused during a 1-minute period at weaning. The former of these two models generates a low concentration of fat in the aortic line, whereas the latter model produces a higher but transient concentration. The in vitro preparation of fat suspensions seemed clinically realistic. The spectrum of fat droplet diameters was similar to what has been measured under clinical conditions of aortic line sampling (28).

Our study clearly showed that the tested Doppler was unable to detect fat droplets. The true input of fat emboli, either soya oil or human wound fat suspension, was visualized by concomitant image analysis. With this design, it was possible to compare the Doppler output signal to the known input of fat emboli, and furthermore, to compare the size and shape distribution of droplets. The Doppler

had built-in software that separated the recorded particles into diameter intervals based on their ultrasonic backscatter. There was a trend towards a dose–response relationship for soya oil, whereas no such correlation was to be found when human fat was tested. Of particular interest, it was shown that the Doppler heavily underestimated the true number of fat particles. This was true also for particles of large diameter, with only ~.02% of fat droplets >20 μm detected. A plausible interpretation suggests that the Doppler only detects fat droplets of considerable size. Such droplets are erroneously classified as small particles by the Doppler software in comparison with the more echo-dense gaseous emboli. According to the manufacturer's documentation, the lower detection limit of air bubbles is 10 μm. Our findings suggest that the detection limit is considerably higher for fat droplets.

The preparation of fat suspensions formed a wide range of particle sizes, dominated by small-diameter droplets. The embolic potential of these droplets was calculated. It was found that the sum of volume contained in particles >10 μm was far greater than the volume of all numerous small droplets. Even so, because of the considerable loss of particle detection regardless of droplet size, this Doppler method must be strongly questioned for this use.

This study is limited from its experimental rather than clinical design. Nevertheless, the aim made prerequisite of an in vitro model to detect fat particles by concomitant Doppler and image analysis. Fat droplets are spherical at zero flow inside the microscopy chamber. The droplets are expected to deform at shear stress, an unknown phenomenon that may affect the comparison between the Doppler signals and the image analysis. Furthermore, our observations suggested that fat droplets remained fairly stable inside the microscopy chamber after preparation. However, droplets may re-structure to form lager-size particles or become dispersed at shear stress, which represent additional unknown factors. A cell-free medium was used rather than blood medium. In fact, with blood vehicle, the background noise increased in the model, possibly reflecting cell aggregates or white blood cells. To what extent the Doppler can discriminate between large-size white blood cells and fat droplets of similar diameter is an intriguing question. A Doppler of higher frequency or of a multifrequency design might have increased the chance of fat detection. The Hatteland Doppler hides unresolved characteristics in terms of glass sphere calibration (19), and furthermore, we confirmed the observation by Eitschberger et al. (19) that the used preparation of glass spheres contains glass dust particles.

In conclusion, it is tempting to use the transcranial Doppler for detection of fat emboli in conjunction with CPB. Our findings strongly suggest that the echogenecity of fat droplets is insufficient for them to be visualized by the used Doppler method.

## ACKNOWLEDGMENTS

This study was supported by grants from the Medical Faculty at Umeå University and the North Sweden Heart Foundation.

## REFERENCES

1. Eagle KA, Guyton RA, Davidoff R, et al. American College of Cardiology; American Heart Association. ACC/AHA 2004 guideline update for coronary artery bypass graft surgery: a report of the American College of Cardiology/American Heart Association Task Force on Practice Guidelines (Committee to Update the 1999 Guidelines for Coronary Artery Bypass Graft Surgery). Circulation. 2004; 110:340–437.
2. Appelblad M, Engstrom G. Fat contamination of pericardial suction blood and its influence on in vitro capillary-pore flow properties in patients undergoing routine coronary artery bypass grafting. J Thorac Cardiovasc Surg. 2002;124:377–86.
3. Challa VR, Moody DM, Troost BT. Brain embolic phenomena associated with cardiopulmonary bypass. J Neurol Sci. 1993;117:224–31.
4. Brooker RF, Brown WR, Moody DM, et al. Cardiotomy suction: a major source of brain lipid emboli during cardiopulmonary bypass. Ann Thorac Surg. 1998;65:1651–5.
5. Fearn SJ, Pole R, Wesnes K, Faragher EB, Hooper TL, McCollum CN. Cerebral injury during cardiopulmonary bypass: emboli impair memory. J Thorac Cardiovasc Surg. 2001;121:1150–60.
6. Roach GW, Kanchuger M, Mangano CM, et al. Adverse cerebral outcomes after coronary bypass surgery. Multicenter Study of Perioperative Ischemia Research Group and the Ischemia Research and Education Foundation Investigators. N Engl J Med. 1996;335:1857–63.
7. Charlesworth DC, Likosky DS, Marrin CA, et al. Northern New England Cardiovascular Disease Study Group. Development and validation of a prediction model for strokes after coronary artery bypass grafting. Ann Thorac Surg. 2003;76:436–43.
8. Bucerius J, Gummert JF, Borger MA, et al. Stroke after cardiac surgery: a risk factor analysis of 16,184 consecutive adult patients. Ann Thorac Surg. 2003;75:472–8.
9. Forteza AM, Koch S, Romano JG, Babikian VL. Detection of microembolus with transcranial Doppler. Rev Neurol. 2000;31:1046–53.
10. Russel D, Brucher R. Online automatic discrimination between solid and gaseous cerebral microemboli with the first multifrequency transcranial Doppler. Stroke. 2002;33:1975–80.
11. Mess WH, Titulaer BM, Ackerstaff RG. A new algorithm for off-line automated emboli detection based on the pseudo-wigner power distribution and the dual gate TCD technique. Ultrasound Med Biol. 2000;26:413–8.
12. Van Zuilen EV, Mess WH, Jansen C, Van der Tweel I, Van Gijn J, Ackerstaff GA. Automatic embolus detection compared with human experts, a Doppler ultrasound study. Stroke. 1996;27:1840–3.
13. Dittrich R, Ringelstein EB. Occurrence and clinical impact of microembolic signals during or after cardiosurgical procedures. Stroke. 2008;39:503–11.
14. Rubens FD, Boodhwani M, Mesana T, Wozny D, Wells G, Nathan HJ. The cardiotomy trial: a randomized, double-blind study to assess the effect of processing of shed blood during cardiopulmonary bypass on transfusion and neurocognitive function. Circulation. 2007; 116:I89–97.
15. Djaiani G, Fedorko L, Borger MA, et al. Continuous-flow cell saver reduces cognitive decline in elderly patients after coronary bypass surgery. Circulation. 2007;116:1888–95.
16. Appelblad M, Engström KG. Fat content in pericardial suction blood and the efficacy of spontaneous density separation and surface adsorption in a prototype system for fat reduction. J Thorac Cardiovasc Surg. 2007;134:366–72.

17. Ogoh S, Dalsgaard MK, Secher NH, Raven PB. Dynamic blood pressure control and middle cerebral artery mean blood velocity variability at rest and during exercise in humans. Acta Physiol (Oxf). 2007;191:3–14.
18. Jonsson P, Karlsson L, Forsberg U, Gref M, Stegmayr C, Stegmayr B. Air bubbles pass the security system of the dialysis device without alarming. Artif Organs. 2007;31:132–9.
19. Eitschberger S, Henseler A, Krasenbrink B, Oedekoven B, Mottaghy K. Investigation on the ability of an ultrasound bubble detector to deliver size measurements of gaseous bubbles in fluid lines by using a glass bead model. ASAIO J. 2001;47:18–24.
20. Wright ES. Sarkozy, Dobell AR, Murphy DR. Fat globulemia in extracorporeal circulation. Surgery. 1963;53:500–4.
21. Caguin F, Carter MG. Fat embolization with cardiotomy, with the use of cardiopulmonary bypass. J Thorac Cardiovasc Surg. 1963;46: 665–72.
22. Moody DM, Brown WR, Challa VR, Stump DA, Reboussin DM, Legualt C. Brain microemboli associated with cardiopulmonary bypass: a histologic and magnetic resonance imaging study. Ann Thorac Surg. 1995;59:1304–7.
23. Jewell AE, Akowuah EF, Suvarna SK, Braidley P, Hopkinson D, Cooper G. A prospective randomised comparison of cardiotomy suction and cell saver for recycling shed blood during cardiac surgery. Eur J Cardiothorac Surg. 2003;23:633–6.
24. de Vries AJ, Gu YJ, Douglas YL, Post WJ, Lip H, van Oeveren W. Clinical evaluation of a new fat removal filter during cardiac surgery. Eur J Cardiothorac Surg. 2004;25:261–6.
25. Svenmarker S, Engström KG, Karlsson T, Jansson E, Lindholm R, Åberg T. Influence of pericardial suction blood retransfusion on memory function and release of protein S100B. Perfusion. 2004;19: 337–43.
26. Eriksson M, Samuelsson E, Gustafson Y, Åberg T, Engström KG. Delirium after coronary bypass surgery evaluated by the organic brain syndrome protocol. Scand Cardiovasc J. 2002;36:250–5.
27. Clayton RH, Pearson DT, Murray A. Clinical comparison of two devices for detection of microemboli during cardiopulmonary bypass. Clin Phys Physiol Meas. 1990;11:327–32.
28. Kaza AK, Cope JT, Fiser SM, et al. Elimination of fat microemboli during cardiopulmonary bypass. Ann Thorac Surg. 2003;75:555–9.